A new methodology to efficiently test pitting corrosion: Design of a 3D printed sample holder to avoid the occurrence of crevice corrosion in chemically aggressive media

Brent Verhoeven,* Maarten Nagels,* Pieter Van Aken,* Roberto Gaggiano,** Barbara Rossi, ***,**** Walter Bogaerts, ***** and Raf Dewil[‡,]*

[‡]Corresponding author. E-mail: raf.dewil@kuleuven.be.

* KU Leuven, Department of Chemical Engineering, Process and Environmental Technology Lab, J. De Nayerlaan 5, 2860 Sint-Katelijne-Waver, Belgium.

** ONDRAF/NIRAS, RD&D Department, Kunstlaan 14, 1210 Brussels, Belgium.

*** KU Leuven, Department of Civil Engineering, Materials and Structures, J. De Nayerlaan 5, 2860 Sint-Katelijne-Waver, Belgium.

**** University of Oxford, Department of Engineering Science, Parks Road, Oxford OX1 3PJ, United Kingdom.

***** KU Leuven, Department of Materials Engineering, Kasteelpark Arenberg 44, 3001 Leuven, Belgium

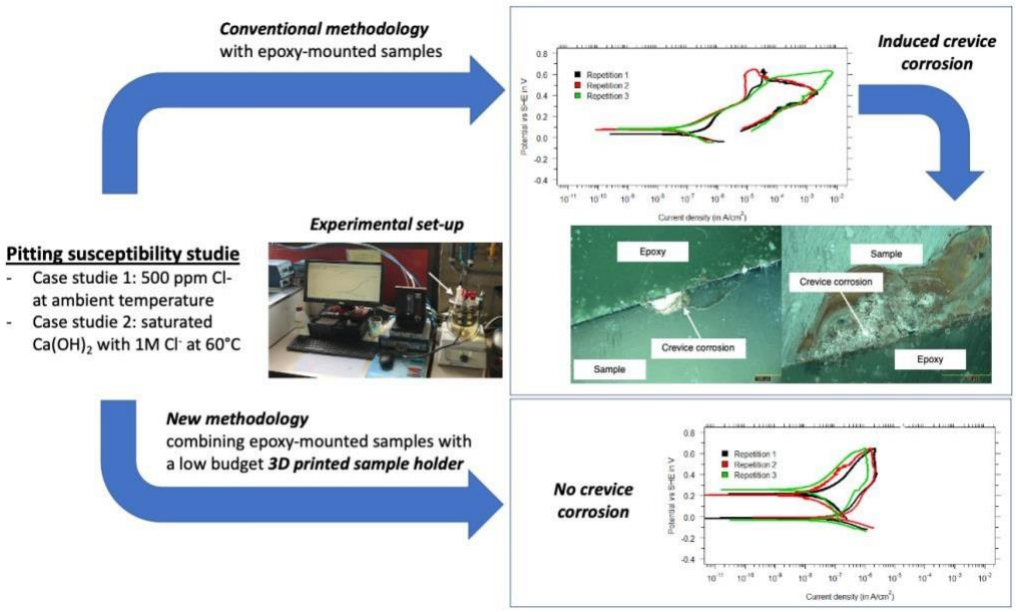
Acknowledgements The authors would like to thank the Belgian Agency for Radioactive Waste and Enriched Fissile Materials (ONDRAF/NIRAS) for the financial support. The Private Foundation De Nayer is kindly thanked for funding the electrochemical potentiostat.

ABSTRACT

Pitting susceptibility of metals in corrosive environment is usually measured using a three-electrode set-up to conduct accelerated corrosion tests. A widely accepted methodology consists in mounting a sample in epoxy-resin and connect it with a copper wire. However, in chloride-rich environments, this often results in the occurrence of crevice corrosion instead of pitting. In this study, a new 3D printed sample holder was designed and its efficiency to study pitting corrosion of metals validated. The new method enables the study of pitting corrosion by improving edge enclosure thus avoiding crevice corrosion. The validation is based on two case studies where stainless steel samples are polarized in (i) 500ppm Cl^- at ambient temperature and (ii) saturated $Ca(OH)_2$ with 1M Cl^- at 60°C. The specifically chosen grade (AISI 316L) shows failure of the electrode clearly initiated at the epoxy-sample edge in traditional tests and poor reproducibility. Results showed that the use of the 3D printed sample holder significantly improved the reliability and efficiency of the testing method, clearly avoiding unrealistic crevice corrosion in the tested conditions. The designed sample holder therefore enables more realistic and representative pitting results in corrosion research opening the possibility of conducting far less expensive repetitive tests.

KEY WORDS: *Chloride; crevice corrosion, pitting; Corrosion rate; aqueous environments; uniform corrosion*

GRAPHICAL ABSTRACT



1 INTRODUCTION

Over the past decades, the susceptibility of metals to corrosion has been a major area of research within the field of material science, and that to avoid premature failure and financial loss in many industrial sectors such as construction and manufacturing ones. Electrochemical lab-scale tests have been fundamental in the scientific understanding of corrosion processes. They provide useful information in a (relatively) short period of time by accelerating the corrosion mechanisms occurring in a defined corrosive electrolyte on a specific (metal) sample. Various techniques have been proposed, including polarization measurements, electrochemical frequency modulation, slow strain rate tests and electrochemical potentiokinetic reactivation. All of them have their own outcomes as well as disadvantages. Potentiodynamic and potentiostatic polarization measurements are key to study pitting susceptibility of metals such as stainless steel in aggressive media [1]. However, the occurrence of crevice corrosion on the working electrode is a common drawback of such methodology. Crevice corrosion can start at lower potential than that required for pitting corrosion, meaning that a metal can be more susceptible to crevice corrosion [2]. Several authors already recognized these problems and proposed several new setups and processes, going from diluted water injection towards prepassivation of the metal coupon or the use of syringe cell [3–8]. Also commercial alternatives for crevice-free working electrodes such as flat specimen holders and Avesta cells are introduced [9, 10]. Unfortunately, these setups are always not cost-effective for executing corrosion tests. For example, Berner et al. proposed the use of Avesta multicells to increase the cost efficiency [11]. Another even more low budget method used epoxy resin to mount the specimen and the resin/specimen interface was painted lacquer to prevent crevice corrosion [12, 13]. Although both studies showed good results, the lacquer is not always sufficient to prevent crevice corrosion. Specific conditions, such as temperature, chloride concentrations and pH, influences the initiation and propagation of crevice corrosion. For example, Han et al. observed the reverse linear relationship between the chloride concentration in the electrolyte and the critical crevice temperature of SAF 2205 DSS [14]. Also, they noticed a dramatical decrease of the critical crevice temperature when the pH was more alkalic. Moreover, Kennel et al. reviewed crevice corrosion models and mentioned that the pH and chloride ion concentration can cause the disruption of the passive film and initiate crevice corrosion [15].

In this study, a new methodology to study pitting corrosion is presented. A low budget 3D printed sample holder is designed to avoid crevice corrosion and critically evaluated in two different environmental conditions with high chloride content. One of these was specifically chosen because the methodology was designed for further studies on pitting corrosion susceptibility of candidate materials for a nuclear disposal concept. Therefore, a concrete pore solution at high pH (12.5), high temperature (60 °C) and high chloride concentration (35 400 ppm) was used.

2 EXPERIMENTAL PROCEDURES

2.1 3D-printed sample holder

The proposed methodology to study pitting corrosion employs a new type of sample holder. Several options were studied and led to the optimal design presented in Fig. 1 where a schematic of the final design of 3D printed sample holder is shown. A more detailed technical drawing is provided in Supplementary Information (Fig. S-1 & Fig. S-2). The sample holder consists of two cylindrical plates that were both printed by a Prusa MK3S 3D printer with a 0.4mm nozzle and 100% infill. The sample holder was printed with a 0.4mm nozzle and 0.2mm layer height. It is recommended to use ABS filament (Acryl Butadiene Styrene) in acid or alkaline solutions. Because of the heavy warping with ABS, the 3D printer was placed inside of an enclosure which helps to control the temperature. PLA filament (Polylactic acid) can be used in less severe electrolytes. A flat rubber gasket (A) is pressed against the cylindrical part (B). The copper wire (C), attached to the epoxy-mounted electrode (D), is inserted into theupper tubular part (E). The sample area of the working electrode (D) is tied against the gasket (C) using nylon M10 bolts (F) and nuts (G). Thread seal tape (PTFE tape) can be used to improve the fixation of the threaded shaft. Hand-tightening the nylon bolts is sufficient to ensure a crevice-free sample area.

2.2 Electrochemical test conditions

Cyclic polarization measurements were conducted to measure uniform corrosion rate and to evaluate the pitting resistance of the chosen metal samples. A Gamry Interface 1010E potentiostat was used to execute the polarization measurements. All tests were performed using a scan rate of 0.167 mV/s [1, 14, 15]. A Ag/AgCl (3.5 M KCl, +205 mV vs SHE) and a Hg/HgO (20% KOH, +98 mV vs SHE) electrode were used as reference electrode in the neutral and alkaline solution, respectively. The scan direction was reversed when the vertex potential or maximal current density (5 mA/cm^2) was achieved [1, 16-17]. After polarization, all samples were checked for local corrosion (pitting or crevice corrosion) by a digital Hirox

KH-8700 microscope.

2.3 Materials and reagents

The following stainless steel grades were used to validate the pitting corrosion tests using the proposed 3D printed sample holder and under the aforementioned test conditions: AISI 316L (1.4404) and DX2205 (1.4462). Both samples were obtained from Outokumpu. The chemical composition and PREN-values (Pitting Resistance Equivalent Number) of the stainless steels are listed in Table 1. It is worth noting that AISI 316L shows failure clearly initiated at the epoxy-sample edge when traditional sample preparation techniques were used. DX2205 was chosen because of its high PREN value and opens the possibility to assess the methodology.

Table 1: Chemical composition of AISI 316L and DX2205 with their PREN-value

Common name	UNS number	Cr (wt%)	Ni (wt%)	Mo (wt%)	C (wt%)	N (wt%)	PREN
AISI 316L	S31603	16-18	10-14	2-3	0.03	0.1	23
DX 2205	S31803	21-23	4.5-6.5	2.5-3.5	0.03	0.08-0.02	31

The samples were embedded in a Technovit® 4071 resin, wet grinded to P600 grit and polished with a polycrystalline diamond suspension (up to 1µm) before performing the cyclic polarization measurements. Two electrolytes were used to validate the sample holder: (i) a solution containing 500 ppm Cl^- (pH=7) at ambient temperature and (ii) a saturated $Ca(OH)_2$ solution containing 35 400 ppm Cl^- (pH=12.5) at 60°C. Chloride contamination was done by adding NaCl to the electrolyte. All used chemicals were ordered at VWR International (Haasrode, Belgium) and test solutions were prepared with Mili-Q water (conductivity <100 µS/cm). To investigate the beneficial effect of the sample holder, two kinds of tests were carried out: with samples mounted in the 3D printed holder and with regular embedded samples (used as reference samples). All tests were repeated three times.

3 RESULTS AND DISCUSSION

3.1 Polarization curves in a NaCl solution with 500 ppm Cl^- at 25°C

The first set of measurements aimed at investigating the effect of the sample holder in a neutral environment. Fig. 2a and 2b compare the polarization plots of AISI 316L (1.4404) without and with the 3D sample holder in 500 ppm Cl^-. Fig. 2a, performed with epoxy-mounted samples, showed strong current increases at 0.45 V, 0.61 V and 0.63 V vs SHE, suggesting that local corrosion is occurring. However, no evidence of crevice corrosion was found via microscopic analysis. This can be explained by the maximal current density (in the hysteresis loop) which was relatively low (< 0.1mA/cm^2). Fig. 2b presents the potentiodynamic measurements of AISI 316L when mounted in the 3D printed sample holder. Interestingly, no strong current increases or hysteresis loops were observed. The absence of hysteresis loops indicates that no local corrosion occurred and that the sample (as working electrode) is protected against crevice corrosion when mounted in the sample holder (compared to traditional epoxy-mounted electrodes). Previous studies have demonstrated that AISI 316L stainless steel has satisfactory pitting resistance in 500 ppm Cl^- containing environments [18–20]. This is in good agreement with the results of the present tests when using the 3D printed sample holder (Fig. 2b), where AISI 316L also shows high pitting resistance in 500 ppm Cl^-. The results without sample holder (Fig. 2a) do not agree with those studies, although, the possible interference of bad edge retention (of the sample) and the occurrence of local corrosion cannot be ruled out.

Fig. 3 displays the polarization curves of DX2205 in a 500 ppm Cl^- solution. No strong current increases in the passive region (300-900 mV vs SHE) were observed. This indicates that epoxy-mounted electrodes and electrodes mounted in the sample holder did not suffer from crevice corrosion. As expected, Epoxy-mounted electrodes in Fig. 3a did not show crevice corrosion mainly because the DX2205 grade has a higher resistance to local corrosion (higher PREN value, see Table 1) [21]. It is known that alloy grades with a higher PREN value also have better resistance to crevice corrosion [22]. Interestingly, the measurements with the sample holder (Fig. 3b) show better reproducibility than the epoxy-mounted samples. The high pitting corrosion resistance of this grade, found in this study, seems to be consistent with other researches [23, 24] which found that DX2205 stainless steel shows excellent pitting corrosion

resistance in NaCl solutions (up to 0.1 M Cl^-). Recently, Huang et. al. [23] reported that no pitting or crevice corrosion was found for DX2205, even for a chloride concentration up to 21 300 ppm Cl^- (epoxy-mounted electrodes). The influence of the sampler holder in the chosen solution is presently not as visible as for the AISI 316L stainless steel grade predominantly because of the higher crevice and pitting corrosion resistance showed by duplex stainless steel grades.

3.2 Polarization curves in a saturated $Ca(OH)_2$ with 35400 ppm Cl^- at 60°C

As a second electrolyte medium, a saturated $Ca(OH)_2$ solution was used. This solution is often used to assess corrosion resistance of stainless steel in a concrete environment for their use as reinforcement bars. To create a harsh testing environment, 35 400 ppm Cl^- was added to the saturated solution and all tests were performed at elevated temperature up to 60°C [24].

The results for an AISI 316L sample mounted in epoxy-resin and with sample holder are compared in Fig. 4. Negative hysteresis loops are observed in Fig. 4a when no loops are present when using a sample holder (Fig. 4b). Furthermore, all measurements carried out in epoxy-resin showed severe attack at the epoxy-sample edge as shown in the microscopic analysis of the samples after the cyclic polarization test (Fig. 5). Numerous pits and crevices were observed on the studied sample area. When evaluating pitting susceptibility of the AISI 316L, possible interferences from crevice corrosion cannot therefore not be ruled out. When using the 3D printed sample holder, oxidizing potentials above oxygen evolution were achieved without strong current increases. This suggests that AISI 316L shows very high pitting corrosion resistance in the tested solution. These results are in agreement with the findings of Elsener et al. [25] who showed no pits on AISI 316L stainless steel even in a 0.1 M NaOH solution (pH 13) containing 177 000 ppm Cl^-. However, some studies report poor pitting resistance of AISI 316L, even at a lower concentration of 354 00 ppm Cl^- [26–29].

Measurements in saturated $Ca(OH)_2$ were also carried out on the DX2205 stainless steel grade. The results of these polarization plots are depicted in Fig. 6. Consistent with the findings for AISI 316L material, it was found that epoxy-mounted samples suffered pitting and crevice corrosion in the studied environment. All polarization tests with epoxy-resin failed due to the occurrence of crevice corrosion. No

pits were detected at the surface of DX2205 stainless steel (Fig. 7), only gaps that initiated at the edge of the mounted sample. However, all measurements with the sample holder showed high pitting resistance of DX2205 in chloride-contaminated saturated $Ca(OH)_2$ at 60°C. These results are consistent with the data obtained at ambient temperature where DX2205 did not pit with 1 M Cl^- [27, 29]. Only few studies such as Mesquita et al. [30] were able to test pitting susceptibility at elevated temperature (pH 10 with 21 240 ppm Cl^- at 50°C) and are in accordance with our findings.

3.3 Uniform corrosion rates determined by Tafel-extrapolation

Tafel-extrapolation is a fundamental technique to estimate the uniform corrosion rate in the tested environments. During the past decade, many corrosion studies [31–37] have used epoxy-mounted electrodes to calculate the corrosion rate. Therefore, it is important that measurements and drawn conclusions based on tests performed with the 3D printed sample holder do not differ from those obtained with epoxy-mounted samples and, in addition, that they result in accurate corrosion rates. Tafel-extrapolation for additional information on the general corrosion behavior were therefore conducted on linear parts of the anodic and cathodic slopes. Table 2 and Fig. 8 provides corrosion potentials for 316L and DX2205 in the tested environments. In Table 3 and Fig. 9, the corrosion rates are summarized. Both parameters were calculated by Tafel-extrapolation, 50-100 mV away from the open-circuit potential [38, 39].

Table 2: Corrosion potentials (in V vs SHE) in 500 ppm Cl^- (pH 7) and sat. $Ca(OH)_2$ with 35 400 ppm Cl^- at 60°C

Material	Corrosion potential in 500 ppm Cl^- (pH 7)		Corrosion potential in saturated $Ca(OH)_2$ with 35 400 ppm Cl^- (pH 12.5)	
(in V vs SHE)	Epoxy-mounted	3D sample holder	Epoxy-mounted	3D sample holder
AISI 316L	0.12±0.007	0.06±0.003	-0.03±0.04	-0.02±0.01
DX2205	0.14±0.02	0.07±0.01	0.06±0.03	-0.03±0.01

Table 3: Tafel-extrapolated corrosion rates in a) 500 ppm Cl^- (pH 7) and b) sat. $Ca(OH)_2$ with 35 400 ppm Cl^- at 60°C

Material	Corrosion rate in 500 ppm Cl^- (pH 7)		Corrosion rate in saturated $Ca(OH)_2$ with 35 400 ppm Cl^- (pH 12.5)	
(in µm/y)	Epoxy-mounted	3D sample holder	Epoxy-mounted	3D sample holder
AISI 316L	0.79 ± 0.24	0.54 ± 0.03	0.75 ± 0.2	0.56 ± 0.13
DX2205	0.67 ± 0.21	0.49 ± 0.03	0.65 ± 0.23	0.78 ± 0.35

In Fig. 9, the general corrosion rates in 500 ppm Cl^- are presented. It is apparent from the bar plot that the stainless steel samples are slowly corroding with rates below 1 µm/y. The standard deviations are much lower when measuring with the sample holder than those obtained with the epoxy-mounted samples. Corrosion rates in saturated $Ca(OH)_2$ are also displayed in Fig. 9. General corrosion rates are still very low (<1 µm/y) but measurements with the sample holder do not show lower standard deviations than epoxy-mounted electrodes, presumably due to the higher working temperature of 60°C.

The corrosion potentials in 500ppm Cl^- and saturated $Ca(OH)_2$ are summarized in Fig. 8. Corrosion potentials measured with epoxy-mounted samples show a higher standard deviation than the results with the sample holder. In Table 3, it is clear that the standard deviation of the tests with the sample holder are often within the same order of magnitude (±0.01). This indicates that tests performed with sample holder show good reproducibility with respect to the corrosion potential. The reason why there is a difference in corrosion potential between the epoxy-mounted electrode and the sample holder is still unclear.

To validate the sample holder combined with the methodology and to verify that the measured uniform corrosion rates do not differ from epoxy-mounted samples, a statistical analysis of the tests was performed in which corrosion rates of the sample holder and the epoxy-mounted samples were compared. First, normality of the measured data (comparing the working electrode procedure) was checked by Kolmogorov-Smirnov normality test [40]. The determined p-values, showed in Table 3, are higher than 0.05 (95% confidence interval), suggesting that the data is following a normal distribution. It is important to check normality because statistical assessment, such as the one-way ANOVA, requires normal

236 distributed data. One-way ANOVA is a statistical assessment enabling to verify if there are any significant
237 differences among the results. In the present study, this method was used to statistically assess the
238 differences among general corrosion rates determined with the sample holder or the epoxy-mounted
239 samples. Table 4 provides the p-values obtained using the one-way ANOVA test for the different materials
240 and test solutions. All p-values are higher than 0.05 which suggests that the general corrosion rates
241 measured with 3D printed sample holder and the epoxy-mounted samples are not statistically different. It
242 can be concluded that the use of a sample holder does not show any influence on the determined uniform
243 corrosion rate when compared to epoxy-mounted samples.

Table 3: P-values of the Kolmogorov-Smirnov test to check normality

Material	p-value of normality test in 500 ppm Cl^-	p-value of normality test in saturated $Ca(OH)_2$ with 35 400 ppm Cl^- (pH 12.5) at 60°C
AISI 316L	0.064	0.15
DX2205	0.089	0.69

Table 4: P-values of the one-way ANOVA to test statistical differences

Material	p-value of ANOVA in 500 ppm Cl^-	p-value of ANOVA in saturated $Ca(OH)_2$ with 35 400 ppm Cl^- (pH 12.5) at 60°C
AISI 316L	0.11	1.98
DX2205	0.22	0.29

4 CONCLUSIONS

The main goals of the current study were to design a new optimized 3D printed sample holder aimed at studying the pitting susceptibility of metals in aggressive electrolytes during cyclic potentiodynamic measurements and to assess whether tests performed using this sampler holder would (1) rule out crevice corrosion usually initiating at the edge of traditional epoxy-embedded sample and (2) provide reliable uniform corrosion results. The main results could be concluded as follows:

(1) This study has shown that epoxy-mounted working electrodes are often not providing reliable pitting corrosion tests in harsh environments. The occurrence of crevice corrosion, initiating at the epoxy-sample edge, makes it impossible to draw reliable conclusions on the pitting susceptibility in predefined conditions and it is therefore recommended to avoid them in metal corrosion research. For example, using traditional epoxy-embedded samples, AISI 316L did show difficulties in the two

different environments, especially in the second one (saturated $Ca(OH)_2$ with 35 400 ppm Cl^-) case, where severe failure of the electrode was observed clearly initiating at the epoxy-sample edge. DX2205 on the contrary only showed small traces of crevices in saturated $Ca(OH)_2$ with 35 400 ppm Cl^-. In 500 ppm Cl^-, no sign of pitting or crevice corrosion were visible (obviously due to the high PREN value) but poor reproducibility was found.

(2) With a 3D printed sample holder, all alloys passed the polarization test, no pitting or crevice corrosion occurred, and reproducibility was remarkably better than the epoxy-mounted samples. And it is important to note that only few studies such as Mesquita et al. [30] were able to test pitting susceptibility at elevated temperature (pH 10 with 21 240 ppm Cl^- at 50°C) and they are in accordance with these findings.

(3) General corrosion rates were also determined by conducting Tafel-extrapolation on the polarization curves. The corrosion potentials determined in tests with a sample holder clearly showed a lower standard deviation and therefore, reproducibility was improved. One-way ANOVA statistical assessment confirmed that the general corrosion rates obtained with the sample holder did not differ from the ones achieved by using the epoxy-mounted samples. It could be concluded that measurements with the sample holder in a 500 ppm Cl^- solution also had a lower standard deviation than regular epoxy-mounted samples. In saturated $Ca(OH)_2$ however, no beneficial effect was observed on the standard deviation, probably due to the higher working temperature of 60°C.

(4) The findings of this study clearly highlight the potential of using the optimized 3D printed sample holder to conduct reliable potentiodynamic measurements where pitting susceptibility can accurately be assessed and providing repeatable uniform corrosion test results. Especially for leaner stainless steel grades i.e. with a lower PREN-value, the implementation of a 3D printed sample holder permits to avoid crevice corrosion at the edge of the epoxy-embedded sample.

DECLARATIONS

Funding The present study is supported by the Belgian Agency for Radioactive Waste and Enriched Fissile Materials (ONDRAF/NIRAS) and the Private Foundation De Nayer.

Conflict of interest The authors have no conflicts of interest to declare that are relevant to the content of this article.

Author contributions Conceptualization: Raf Dewil, Walter Bogaerts, Barbara Rossi; Methodology: Brent Verhoeven, Maarten Nagels, Walter Bogaerts; Formal analysis and investigation: Brent Verhoeven, Maarten Nagels; Writing – original draft preparation: Brent Verhoeven, Pieter Van Aken; Writing – review and editing: Pieter Van Aken, Roberto Gaggiano, Barbara Rossi, Walter Bogaerts, Raf Dewil; Funding Acquisition: Raf Dewil, Walter Bogaerts; Supervision: Robberto Gaggiano, Raf Dewil, Walter Bogaerts

REFERENCES

1. Esmailzadeh S, Aliofkhazraei M, Sarlak H (2018) Interpretation of Cyclic Potentiodynamic Polarization Test Results for Study of Corrosion Behavior of Metals: A Review. Prot Met Phys Chem Surf 54:976–989. https://doi.org/10.1134/S207020511805026X
2. Galvele JR (2005) Tafel's law in pitting corrosion and crevice corrosion susceptibility. Corros Sci 47:3053–3067. https://doi.org/10.1016/j.corsci.2005.05.043
3. Song G-L, Xu Z (2012) Crystal orientation and electrochemical corrosion of polycrystalline Mg. Corros Sci 63:100–112. https://doi.org/10.1016/j.corsci.2012.05.019
4. Zhang J, Yuan J, Qiao Y, et al (2003) The corrosion and passivation of SS304 stainless steel under square wave electric field. Mater Chem Phys 79:43–48. https://doi.org/10.1016/S0254-0584(02)00445-5
5. Shen J, Song G, Zheng D, Wang Z (2019) A double-mode cell to measure pitting and crevice corrosion. Mater Corros 70:2228–2237. https://doi.org/10.1002/maco.201910932
6. ASTM G150-13 (2013) Standard Test Method for Electrochemical Critical Pitting Temperature Testing of Stainless Steels. ASTM International, West Conshohocken
7. Vanegas, M. ; Wang, K. ; Iannuzzi, M. Technical Note: Methodology Development to Study Two-Dimensional Stainless Steel Pitting Corrosion Mechanisms Using Foil Samples. CORROSION (2022) 78 (6): 473-478. https://doi.org/10.5006/4057
8. Panindre, A.M; Frankel, G.S. Technical Note: Electrochemical Testing for Pitting Corrosion Above Ambient Temperatures Using the Syringe Cell. CORROSION (2021) 77 (9): 1025–1028. https://doi.org/10.5006/3854
9. Ovarfort R (1988) New electrochemical cell for pitting corrosion testing. Corros Sci 28:135–140. https://doi.org/10.1016/0010-938X(88)90090-X
10. Husain A, Brahme PS, Al-Shamali O (2007) Development of a modified test cell for AC impedance testing of coated Al fins. J Coat Technol Res 4:317–325. https://doi.org/10.1007/s11998-007-9043-y
11. Berner M, Liu H-P, Olsson C-OA (2008) Estimating localised corrosion resistance of low alloy stainless steels: comparison of pitting potentials and critical pitting temperatures measured on lean duplex stainless steel LDX 2101 after sensitation. Corros Eng Sci Techn 43:111–116. https://doi.org/10.1179/174327808X286347
12. Ghayad IM, Hamada AS, Girgis NN, Ghanem W (2004) Effect of cold working on the aging and corrosion behavior of Fe-Mn-Al stainless steel. Nice, France, p 10
13. Cardoso JL, Silva Nunes Cavalcante AL, Araujo Vieira RC, et al (2016) Pitting corrosion resistance of austenitic and superaustenitic stainless steels in aqueous medium of NaCl and H_2SO_4. J Mater Res 31:1755–1763. https://doi.org/10.1557/jmr.2016.198
14. Han D, Jiang YM, Shi C, et al (2012) Effect of temperature, chloride ion and pH on the crevice corrosion behavior of SAF 2205 duplex stainless steel in chloride solutions. J Mater Sci 47:1018–1025. https://doi.org/10.1007/s10853-011-5889-6

15. Kennell GF, Evitts RW, Heppner KL (2008) A critical crevice solution and IR drop crevice corrosion model. Corros Sci 50:1716–1725. https://doi.org/10.1016/j.corsci.2008.02.020
16. ASTM G61-86 (2018) Standard Test Method for Conducting Cyclic Potentiodynamic Polarization Measurements for Localized Corrosion Susceptibility of Iron-, Nickel-, or Cobalt-Based Alloys. ASTM International, West Conshohocken
17. ASTM G5-94 (2004) Standard Reference Test Method for Making Potentiostatic and Potentiodynamic Anodic Polarization Measurements. ASTM International, West Conshohocken
18. Somrerk CA, Wachirasiri W, Lothongkum G (2013) Effects of Chloride and Sulphate Ions on the Experimental E-pH Diagrams of AISI 316L Stainless Steel in Deaerated Aqueous Solutions. Adv Mat Res 813:443–446. https://doi.org/10.1002/maco.201910932
19. Lothongkum G, Vongbandit P, Nongluck P (2006) Experimental determination of E-pH diagrams for 316L stainless steel in air-saturated aqueous solutions containing 0-5,000 ppm of chloride using a potentiodynamic method. Anti-corros Method M 53:169–174. https://doi.org/10.1108/00035590610665581
20. Refaey SAM, Taha F, Abd Al-Malak AM (2006) Corrosion and Inhibition of 316L stainless steel in neutral medium by 2-Mercaptobenzimidazole. Int J Electrochem Sci. https://doi.org/10.20964/1020080
21. King F (2009) Corrosion Resistance of Austenitic and Duplex Stainless Steels in Environments Related to UK Geological Disposal. Quintessa Limited, Oxfordshire, United Kingdom
22. Olssen CAO (2018) Wet Corrosion of Stainless Steels and Other Chromium-Bearing Alloys," in Encyclopedia of Interfacial Chemistry: Surface Science and Electrochemistr. In: Encyclopedia of Interfacial Chemistry: Surface Science and Electrochemistry. Elsevier, pp 535–542
23. Huang T-S, Tsai W-T, Pan S-J, Chang K-C (2018) Pitting corrosion behaviour of 2101 duplex stainless steel in chloride solutions. Corros Eng, Sci Techn 53:9–15. https://doi.org/10.1080/1478422X.2017.1394020
24. Klapper HS, Stevens J, Wiese G (2013) Pitting Corrosion Resistance of CrMn Austenitic Stainless Steel in Simulated Drilling Conditions—Role of pH, Temperature, and Chloride Concentration. Corrosion 69:1095–1102. https://doi.org/10.5006/0947
25. Elsener B, Addari D, Coray S, Rossi A (2011) Stainless steel reinforcing bars - reason for their high pitting corrosion resistance. Mater Corros 62:111–119. https://doi.org/10.1002/maco.201005826
26. Gastaldi M, Bertolini L (2014) Effect of temperature on the corrosion behaviour of low-nickel duplex stainless steel bars in concrete. Cement Concrete Res 56:52–60. https://doi.org/10.1016/j.cemconres.2013.11.004
27. Moser RD, Singh PM, Kahn LF, Kurtis KE (2012) Chloride-induced corrosion resistance of high-strength stainless steels in simulated alkaline and carbonated concrete pore solutions. Corros Sci 57:241–253. https://doi.org/10.1016/j.corsci.2011.12.012
28. Blanco G, Bautista A, Takenouti H (2006) EIS study of passivation of austenitic and duplex stainless steels reinforcements in simulated pore solutions. Cement Concrete Comp 28:212–219. https://doi.org/10.1016/j.cemconcomp.2006.01.012
29. Paredes EC, Bautista A, Alvarez SM, Velasco F (2012) Influence of the forming process of corrugated stainless steels on their corrosion behaviour in simulated pore solutions. Corros Sci 58:52–61. https://doi.org/10.1016/j.corsci.2012.01.010
30. Mesquita TJ, Chauveau E, Mantel M, et al (2012) Lean duplex stainless steels—The role of molybdenum in pitting corrosion of concrete reinforcement studied with industrial and laboratory castings. Mater Chem Phys 132:967–972. https://doi.org/10.1016/j.matchemphys.2011.12.042
31. Saadawy M (2012) Kinetics of Pitting Dissolution of Austenitic Stainless Steel 304 in Sodium Chloride Solution. ISRN Corros 2012:1–5. https://doi.org/10.5402/2012/916367
32. Alonso-Falleiros N, Wolynec S (2002) Correlation between Corrosion Potential and Pitting Potential for AISI 304L Austenitic Stainless Steel in 3.5% NaCl Aqueous Solution. Mater Res 5:77–84. https://doi.org/10.1590/S1516-14392002000100013
33. Xu C, Zhang Y, Cheng G, Zhu W (2008) Pitting corrosion behavior of 316L stainless steel in the

media of sulphate-reducing and iron-oxidizing bacteria. Mater Charact 59:245–255. https://doi.org/10.1016/j.matchar.2007.01.001
34. He L, Wang Y, Singh PM (2017) Pitting Behavior of Lean Duplex Stainless Steels in Thiosulfate-Containing Paper Machine Environment. New Orleans, United States of America
35. Shet N, Nazareth R, Suchetan PA (2019) Corrosion inhibition of 316 stainless steel in 2M HCl by 4-{[4-(dimethylamino)benzylidene]amino}-5-methyl-4H-1,2,4-triazole-3-thiol. Chemical Data Collections 20:100209. https://doi.org/10.1016/j.cdc.2019.100209
36. Abdallah M, Salem MM, Al Jahdaly BA, et al (2017) Corrosion Inhibition of Stainless Steel Type 316 L in 1.0 M HCl Solution Using 1,3-Thiazolidin-5-one Derivatives. Int J Electrochem Sci 12:4543–4562. https://doi.org/10.20964/2017.05.35
37. Abdallah M, Hazazi OA, Fouda AS, Abdel-Fatah A (2015) Corrosion inhibition of stainless steel type 316L in hydrochloric acid solution using p-aminoazobenzene derivatives. Prot Met Phys Chem Surf 51:473–480. https://doi.org/10.1134/S2070205115030028
38. Stansbury EE, Buchanan RA (2000) Fundamentals of electrochemical corrosion. ASM International, Materials Park, OH
39. Kelly RG (2003) Electrochemical techniques in corrosion science and engineering. Marcel Dekker, New York
40. Lopes RHC (2011) Kolmogorov-Smirnov Test. In: International encyclopedia of statistical science. Springer, Berlin, Germany, pp 718–720

FIGURE CAPTIONS

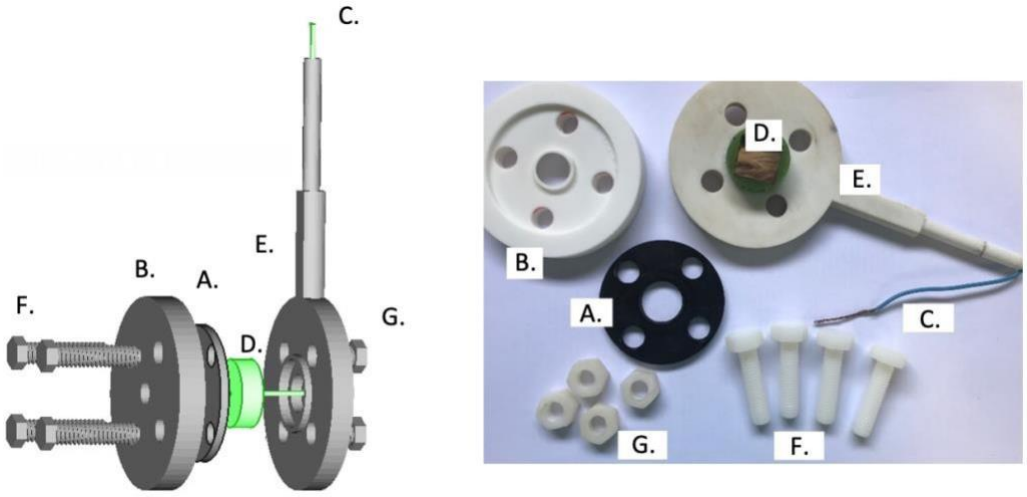
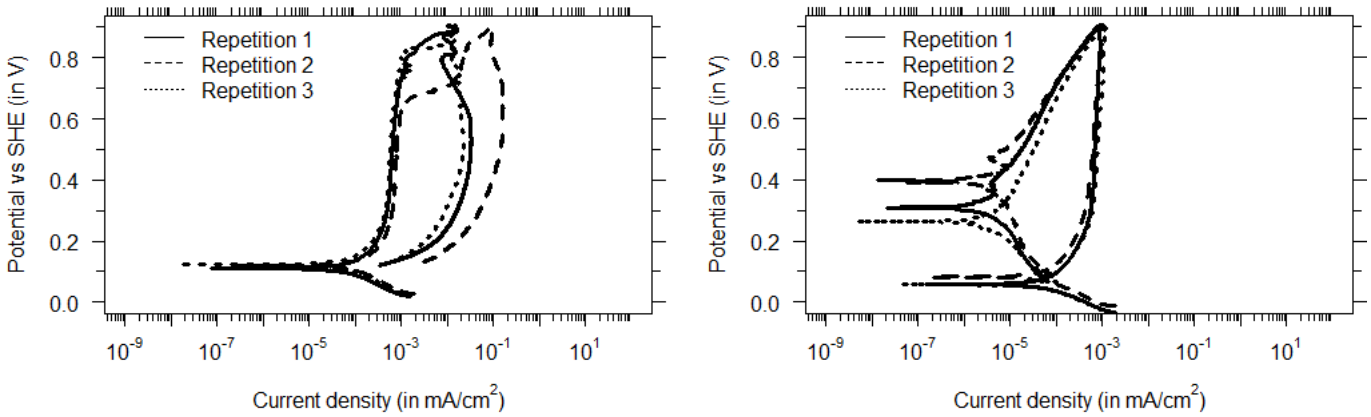
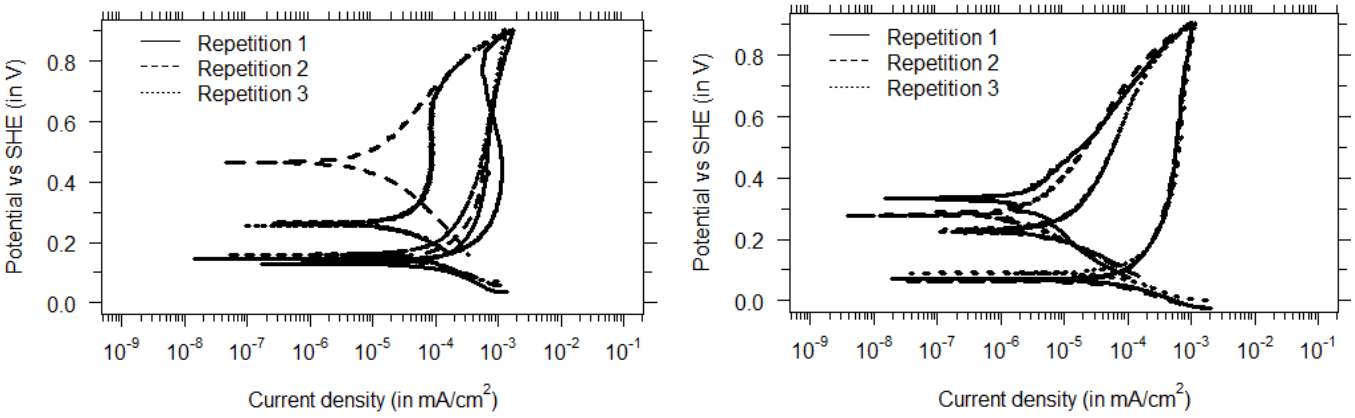


Fig. 1: Simplified technical drawing of the 3D printed sample holder. It consists of (A) rubber gasket 4 nylon M10 bolts (B) Cylindrical 3D printed part 3D printed bottom part (C) copper wire of the working electrode (D) epoxy-mounted working electrode (Ø 30mm) with attached copper wire (not part of the sample holder as such) (E) 3D printed upper tubular part (F) 4 nylon M10 bolts (G) 4 nylon M10 nuts.



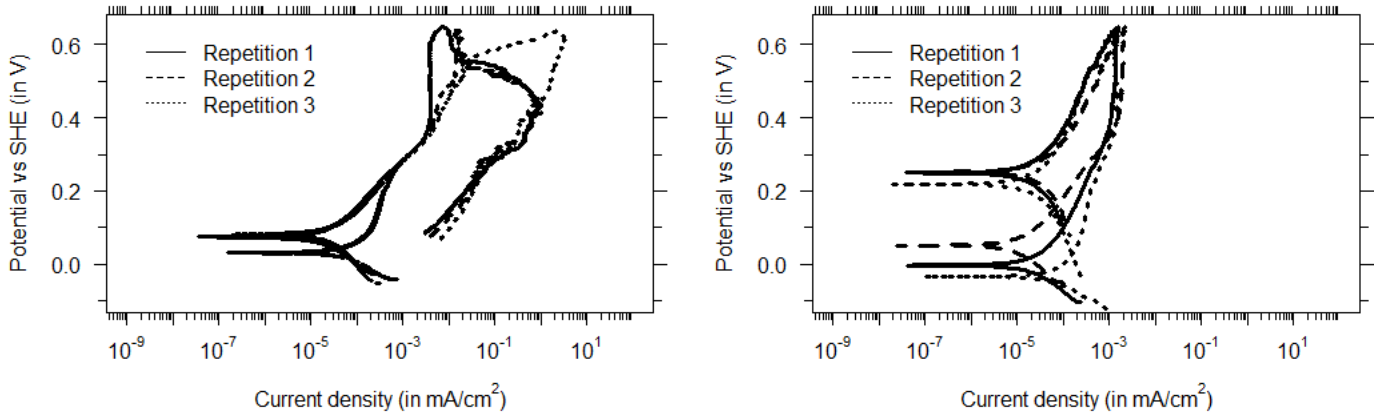
A) B)

Fig. 2: Potentiodynamic polarization plots of AISI 316L with 500 ppm Cl^- A) in epoxy-resin and B) with a 3D-printed sample holder.



A) B)

Fig. 3: Potentiodynamic polarization plots of Duplex 2205 with 500 ppm Cl- A) in epoxy-resin and B) with a 3D-printed sample holder.



A) B)

Fig. 4: Potentiodynamic polarization plots of AISI 316L in saturated $Ca(OH)_2$ at 60°C with 1M Cl^- A)in epoxy-resin and B) with a 3D printed sample holder.

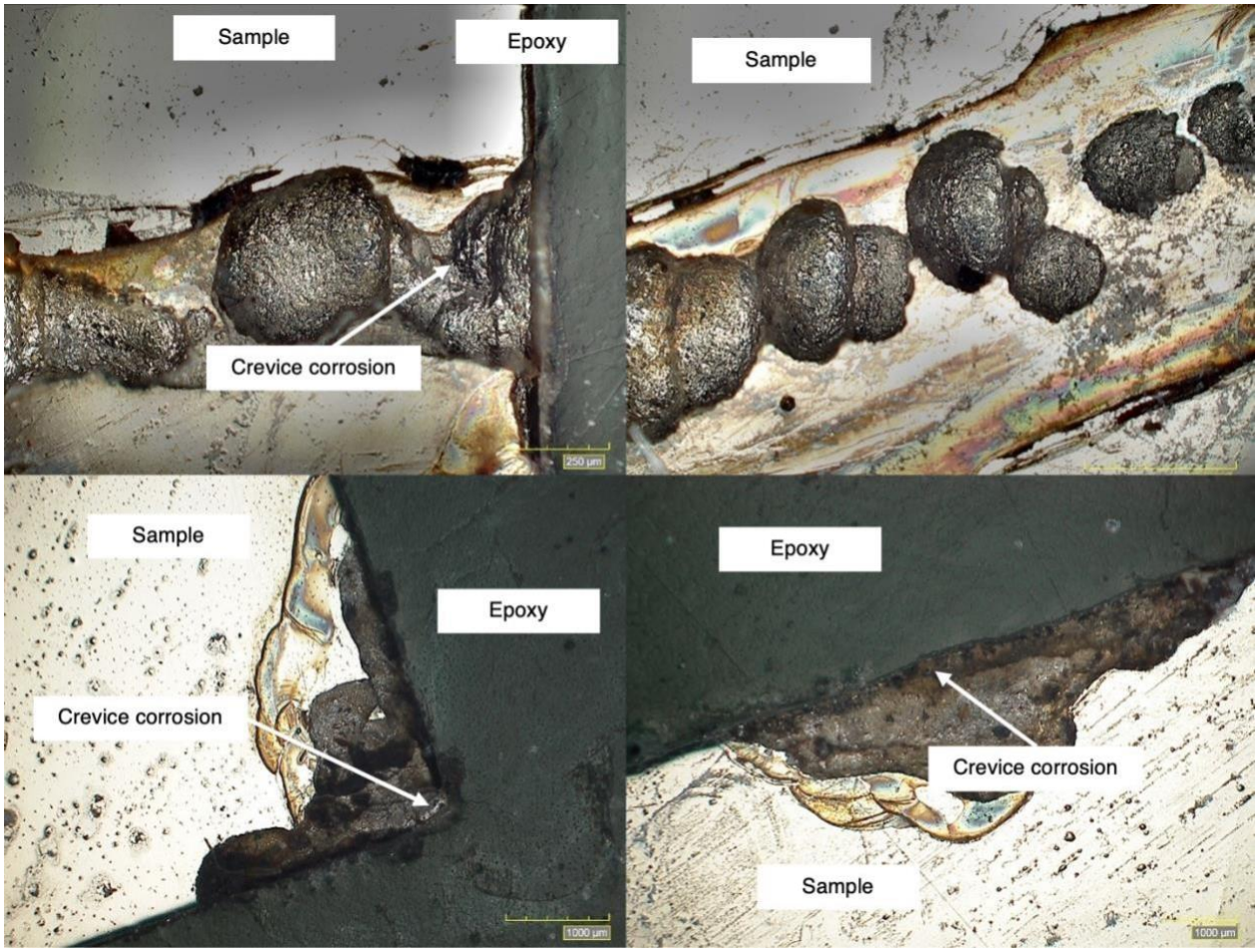
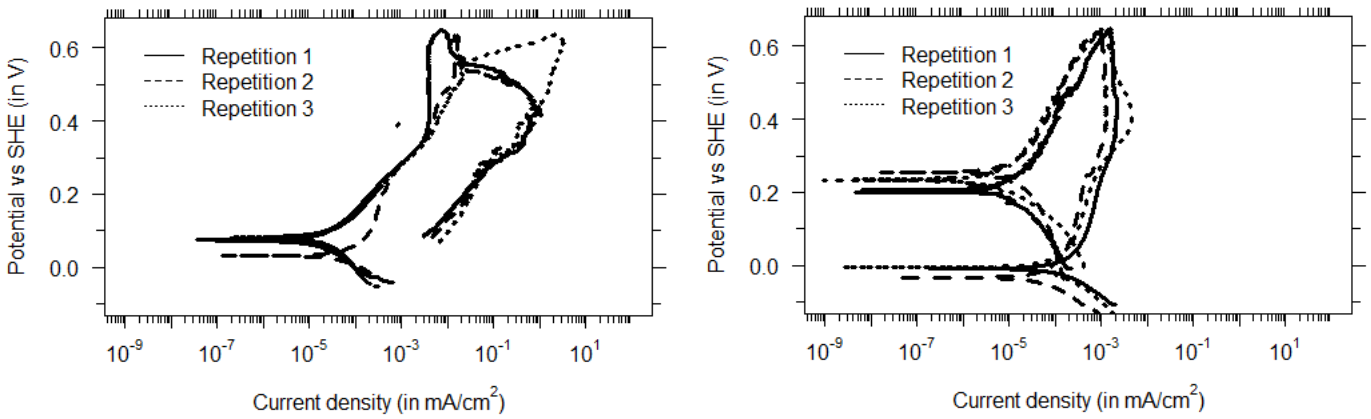


Fig. 5: Crevice corrosion initiated on AISI 316L in saturated $Ca(OH)_2$ with 35 400ppm Cl^- in epoxy-resin (i.e. without a 3D printed sample holder).



A) B)

Fig. 6: Potentiodynamic polarization plots of Duplex 2205 in saturated $Ca(OH)_2$ at 60°C with 35400ppm Cl^- A) in epoxy-resin and B) with a 3D-printed specimen holder.

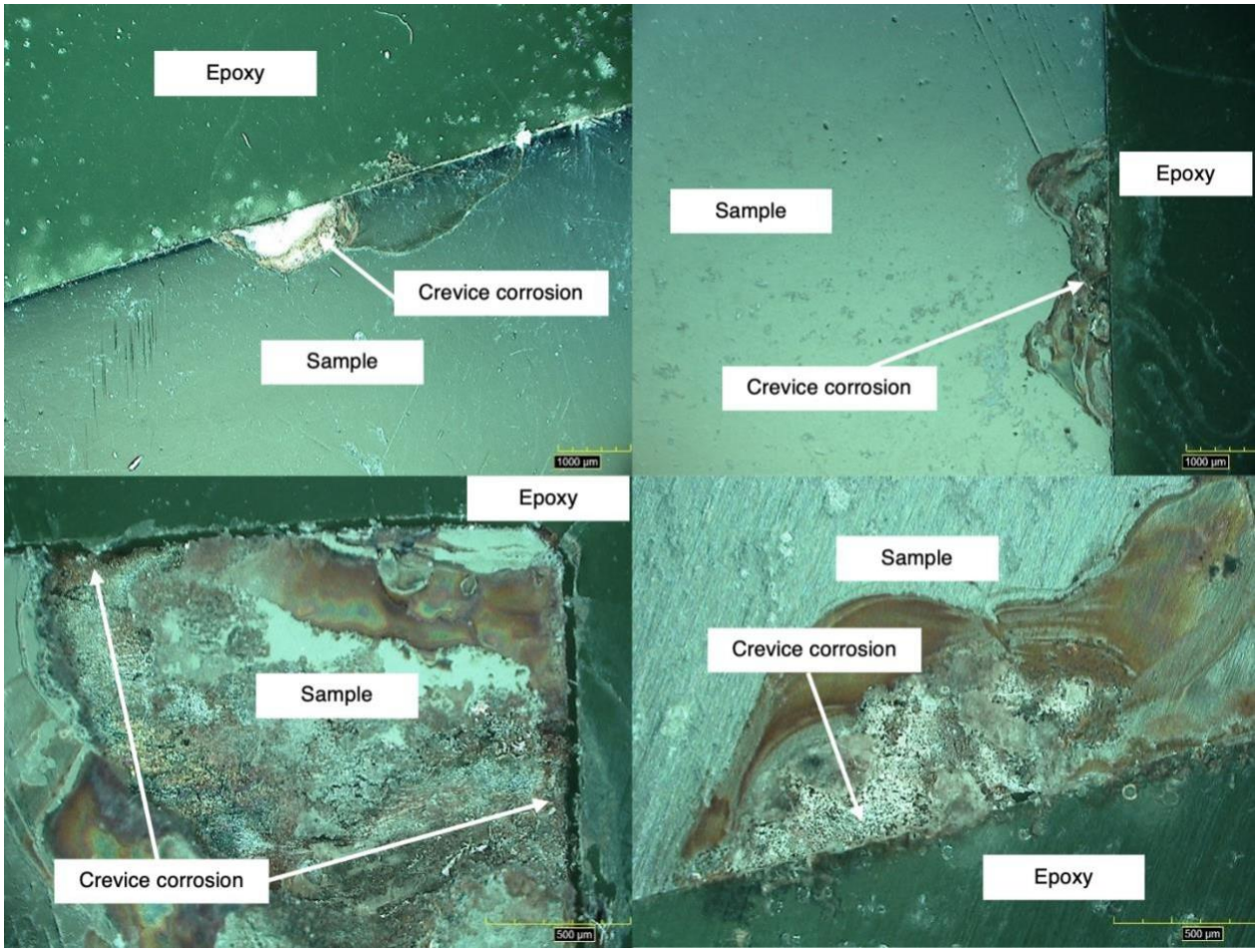


Fig. 7: Crevice corrosion initiated on Duplex 2205 in saturated $Ca(OH)_2$ with 35 400ppm Cl^- in epoxy-resin (i.e. without a 3D printed sample holder).

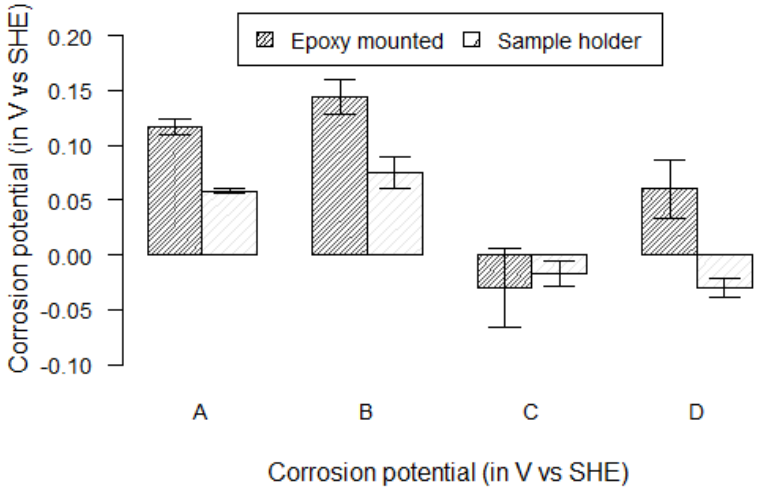


Fig. 8: Corrosion potentials determined by Tafel-extrapolation in: A) 500 ppm Cl^- for AISI 316L B) 500 ppm Cl^- for DX2205 C) sat. $Ca(OH)_2$ with 35000ppm Cl^- for AISI 316L at 60°C and D) sat. $Ca(OH)_2$ with 35000ppm Cl^- for DX2205 at 60°C

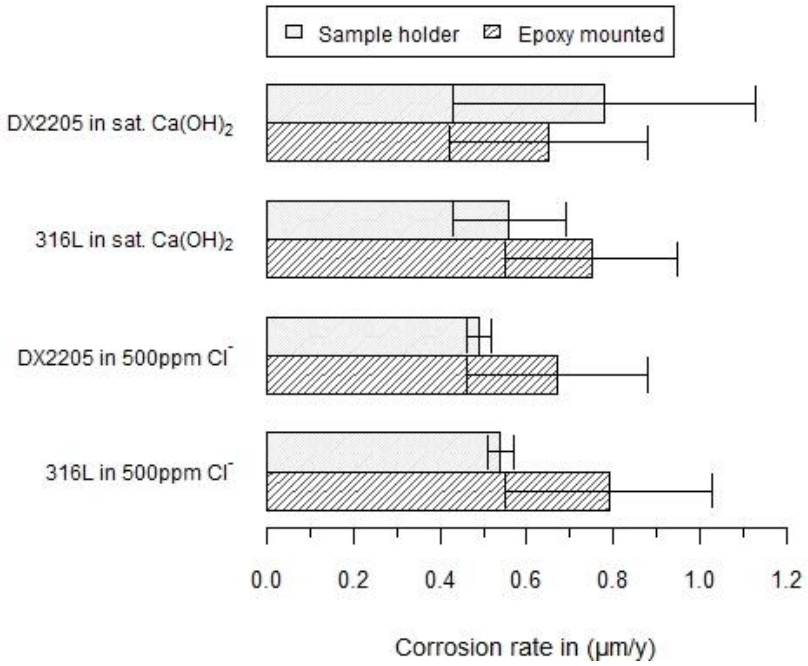


Fig. 9: Uniform corrosion rates determined by Tafel-extrapolation in 500 ppm Cl^- (pH 7) and sat. $Ca(OH)_2$ with 35 400 ppm Cl^- at 60°C.